155 DOPPLER RADAR AND STORM ENVIRONMENT OBSERVATIONS OF A MARITIME TORNADIC SUPERCELL IN SYDNEY, AUSTRALIA

Harald Richter*, Alain Protat
Research and Development Branch, Bureau of Meteorology, Melbourne, Australia

James Taylor
Extreme Weather Desk, Bureau of Meteorology, Melbourne, Australia

Joshua Soderholm
Climate Research Group, University of Queensland, Brisbane, Australia

1. INTRODUCTION

During the late morning of 16 December 2015 an EF-2 tornado (for information on the Enhanced Fujita Scale, see http://www.spc.noaa.gov/efscale/) occurred at a distance of 4 km southeast of Australia's busiest airport in Sydney. This tornado was notable in many ways. A relative abundance of observations was available, including scans from the operational Kurnell C-band Doppler radar located less than 2 km from the tornado path. The parent supercell tracked over water just off the east Australian coast during its entire life cycle, apart from a brief period when it crossed the Kurnell peninsula during the time when the observed tornado occurred. The tornado passed over an Automatic Weather Station (AWS) located on a jetty inside Botany Bay which recorded a wind gust of 59.2 m s^{-1} (213 km hr^{-1}, 115 kts) at 23:33 UTC (10:33 am local time). The three second wind gust measured by the Kurnell AWS is an Australian record outside of a tropical cyclone.

The parent storm exhibited several rear-flank downdraft (RFD) pulses and strong gate to gate velocity couplets prior to the Kurnell tornado (not shown), suggestive of a potentially cyclic tornado producer over the ocean waters south of Sydney, especially when viewed in the context that the RFD was relatively warm (ΔT ~ 4 K, where ΔT is the surface temperature difference between the sampled RFD air and the environmental air) when sampled at Bellambi (south of Sydney) at 2215 UTC, a bit over an hour prior to the Kurnell tornado

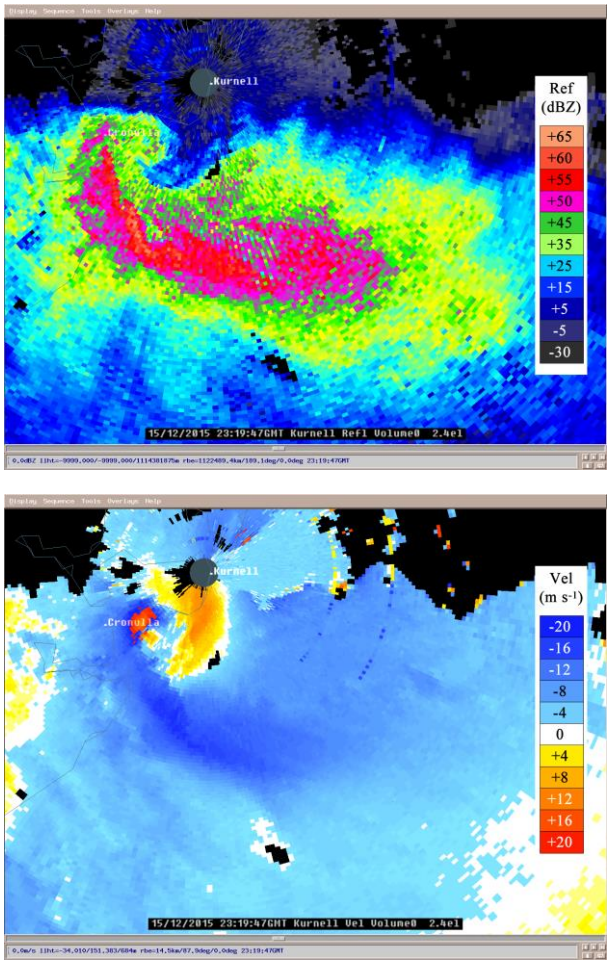

Fig. 1: Kurnell C-band Doppler radar imagery at 2319 UTC 15 December 2015 (10:19 am LT 16 Dec 2015) at 2.4° elevation; reflectivity (top image) and radial velocity (bottom image).

(Markowski 2002; Markowski et al. 2008; Markowski and Richardson 2014).

Damage from the tornado was extensive with the Insurance Council of Australia reporting it to be the most costly disaster of the Australian

*Corresponding author address: Harald Richter, Research and Development Branch, Bureau of Meteorology, PO Box 1289K, Melbourne VIC 3001, Australia; e-mail: h.richter@bom.gov.au.

2015/2016 summer, costing insurance companies AU$206m.

Fig. 1 illustrates the HP supercell storm structure around the time of tornado onset (Moller et al. 2003), while Fig. 2 shows the approximate path of the parent storm, a sample of its damage path and a snippet of the visual appearance of the largely rain-obscured tornado funnel.

This paper describes our initial exploration of the observational data available for this storm. The aims are to show why the environment supported a tornadic storm early in the day and so close to the ocean, and to document some details of the storm's structure.

Fig. 2: Approximate supercell storm track from 2130 UTC 15 December to 0030 UTC 16 December (left) ; Tornado damage at Kurnell (center) and enhanced still frame from a video showing the left edge of the tapered tornado funnel (right; Courtesy of Peter Grassmayr).

2. KINEMATIC ASSESSMENT OF THE MESOCYCLONE AND THE TORNADO CYCLONE

Dual Doppler winds were derived using the Terry Hills S-band Doppler radar (~36 km to the north of Kurnell) and the Kurnell radar (1.6 km to the east of tornado track) based on the methodology described in Protat and Zawadzki (1999) and Collis et al. (2013). The tornado parent cyclone at 2.5 km AGL appears as a zone of convergence in the southwest corner of a ~7 km wide low-level mesocyclone (Fig. 3).

Just prior to tornado formation the storm ingested localised patches of enhanced 0.2-1 km storm-relative helicity (SRH; Fig. 4; Davies-Jones 1984). The key contributor to the overall SRH values appears to be a 'vorticity sheet' within the storm's inflow layer where the north-easterly inflow backs to a north-westerly flow (Fig. 5).

Aircraft Meteorological Data Relay (AMDAR) hodographs taken from three flights at 2256 UTC, 2258 UTC and 2311 UTC (Fig. 6) confirm very strong spatiotemporal variability in the SRH (Fig. 7).

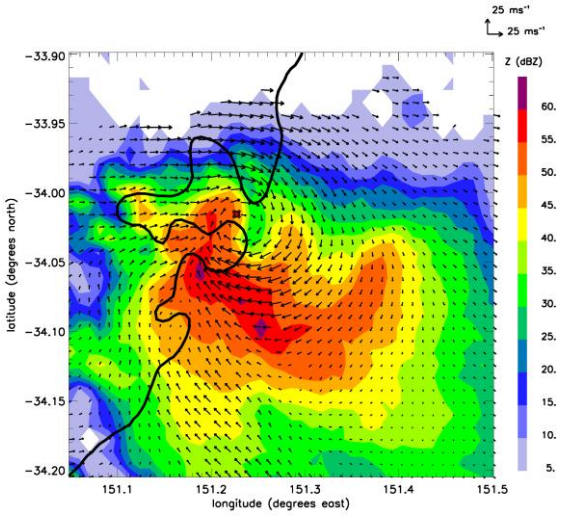

Fig. 3: Dual Doppler winds at 2331 UTC at 2.5 km AGL. Color fill is the corresponding reflectivity from the Kurnell radar. Winds shown as vectors with increased length corresponding to increased speed.

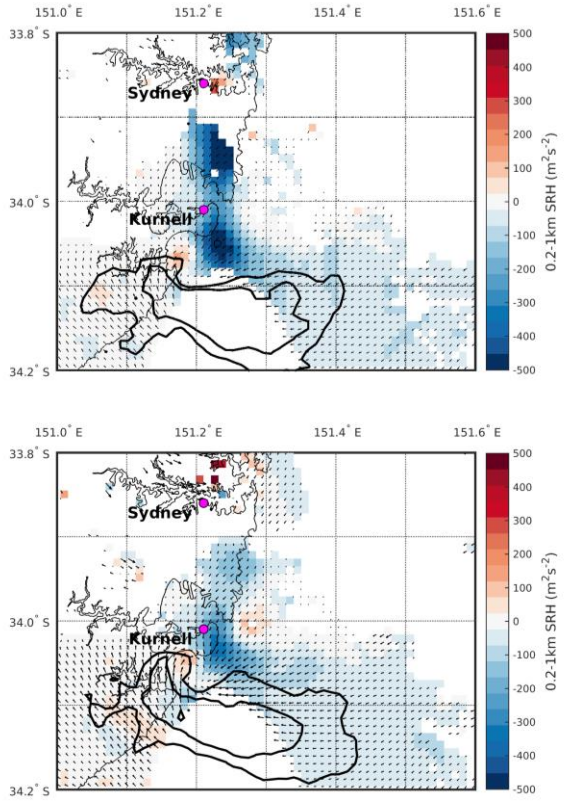

Fig. 4: 0.2-1 km AGL storm-relative helicity (shaded) based on the dual Doppler-derived wind profile. Wind vectors are shown at 500 m AGL and also derived from dual Doppler data. Storm motion (subjectively determined from Kurnell radar data around tornado time) used is 7.5 m s^{-1} towards 19 degrees. Bold contours show smoothed 35, 45, and 55 dBZ outlines at 500 m AGL. The times shown are 2313 UTC (top) and 2319 UTC (bottom).

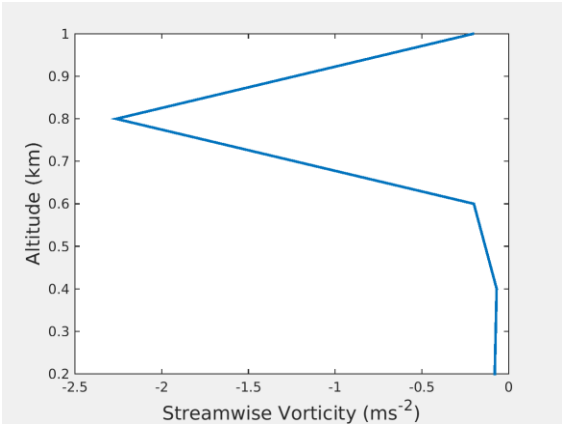

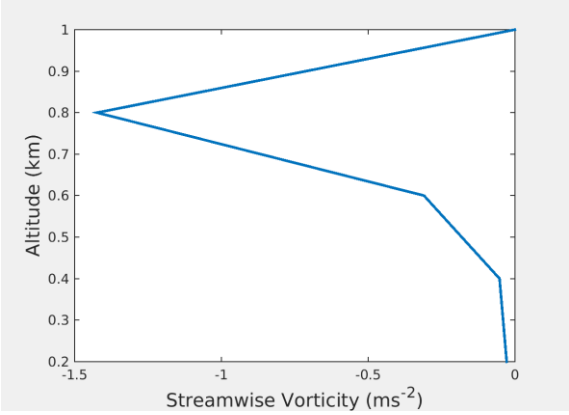

Fig. 5: Vertical profile of the streamwise vorticity at 2313 UTC (upper panel) and 2319 (lower panel) taken at the locations of the respective 0.2-1 km SRH maxima shown in Figure 4 (southern maximum at the location of the hollow black circle in the first and center of the SRH maximum southeast of Kurnell in the second panel).

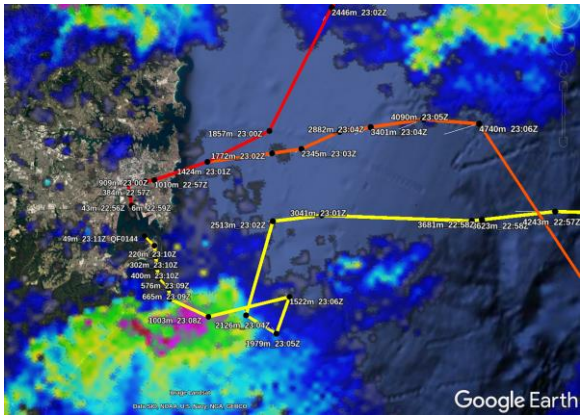

Fig. 6: Sydney airport AMDAR flight paths with height and time overlaid on the 2306 UTC radar reflectivity from the Terry Hills radar. Flight tracks: red is 2256 UTC ascending; orange is 2258 UTC ascending; yellow is 2311 UTC descending.

The 2311 UTC flight took place about 10 km to the south and 15 minutes after the other two flights. It sampled a profoundly different wind field with 0-1 km SRH values increased three- to fourfold (estimated based on Fig. 7). Unlike the earlier two flights, the 2311 UTC flight sampled the storm inflow region northeast of the updraft during its lowest ~700 m of while descending, so its SRH sampling is more informative of the actual storm-relative helicity ingested by the storm.

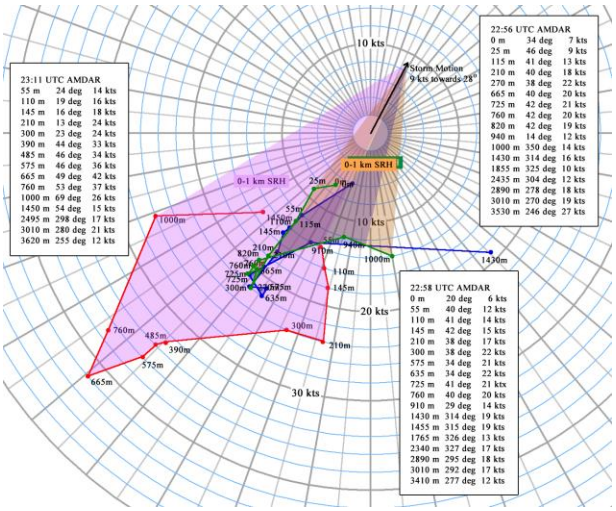

Fig. 7: Observed hodographs based on the 22:56 UTC (green), 22:58 UTC (blue) and 23:11 UTC (red) AMDARS shown in Fig. 6.

3. THERMODYNAMIC ASSESSMENT OF THE STORM ENVIRONMENT

A curiosity about this case study is the appearance of a tornadic supercell linked to a commonly capped marine boundary layer and many hours prior to the peak in diurnal heating (around 10:30 am LT instead of the afternoon). This section begins to explore why the tornadic storm occurred when and where it did from a thermodynamic point of view.

Fig. 8 shows the best available regular radiosonde sounding available at 19 UTC at Sydney airport (black ascent curves). As expected a firm capping inversion is apparent around 600-800 m AGL with easterly onshore flow below it. The 1-hour ACCESS-R model forecast shows skill in capturing this sharp inversion at the correct height level (red curve in Fig. 8).

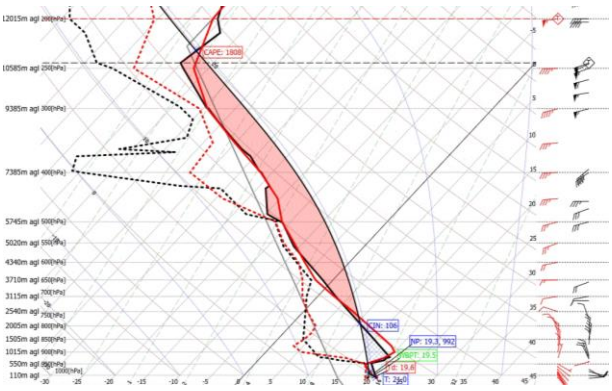

Fig. 8: 18 UTC 15 December 2015 ACCESS-R (red) model sounding and 19 UTC 15 December observed Sydney Airport radiosonde sounding (black).

Fig. 9 shows that the ACCESS-R model maintained its skill in producing a credible thermal profile near the tornadic supercell at 2300 UTC prior to the tornado (right member of the twin red curve). The model profile compares well with the three AMDAR profiles taken at 2256 UTC, 2258 UTC and 2311 UTC near Sydney Airport.

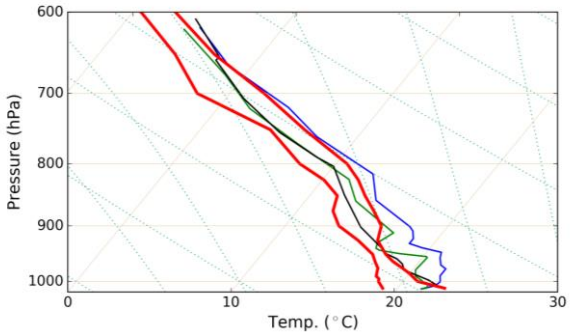

Fig. 9: Sydney airport soundings based on a 6-hour forecast from the 18 UTC ACCESS-R run valid at 23 UTC (red; both temperature and dew point temperature are shown), the 2256 UTC AMDAR (blue), the 2258 UTC AMDAR (green) and the 2311 UTC AMDAR (black);

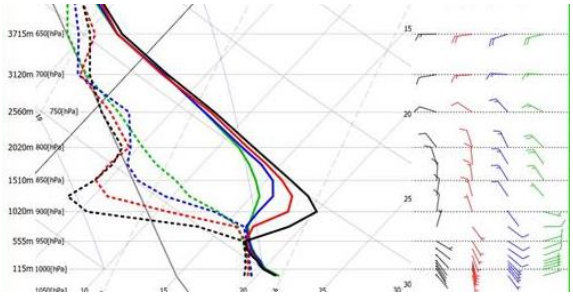

Fig. 10: Hourly model soundings at 18 UTC (black), 19 UTC (red), 20 UTC (blue) and 21 UTC (green) based on the 18 UTC run of ACCESS-R indicating the rapid removal of the inversion prior to the Kurnell tornado at ~2330 UTC.

With the credibility of the ACCESS-R thermal profile at Sydney Airport strengthened between 19-23 UTC, Fig. 10 shows a gradual cooling and moistening of the Sydney Airport sounding between 18 UTC and 21 UTC. The firmly capped marine layer at 18 UTC experienced complete cap removal during the early morning hours (between 19-23 UTC or 6 am and 10 am LT; Figs. 9, 10) through cooling and moistening of the atmosphere *above* the marine boundary layer (around 900

hPa). Early exploration of the thermal advection in the model and observational data such as radar (not shown) points towards a potential role of evaporating light precipitation from high-based cloud in the cooling and moistening of the capping layer. A second candidate mechanism is ascent along isentropic surfaces as indicated by the most recent ACCESS-R model runs.

SUMMARY

On 16 December 2015 an EF-2 tornado crossed a small Peninsula just 4 km southeast of Sydney Airport. A wind gust of 59 m s^{-1} was measured as the tornado moved offshore along the northern coastline of the Peninsula, and substantial damage occurred to a number of buildings.

Based on a dual-Doppler wind analysis, small confined patches of large low-level storm-relative helicity (SRH) are evident along the eastern coastline of Australia just ahead of the storm and prior to the Kurnell tornado. In the vertical, these maxima in low-level SRH are dominated by a "sheet" of large streamwise vorticity along the interface of north-easterly flow (below) and north-westerly flow (above).

Early in the morning of 16 December 2015 a strong capping inversion was in place near the location of the future tornadic storm. This cap eroded over a period of just a few hours during the morning. A possible explanation for the rapid cap removal is high-based pre-existing light showers raining into a very dry capping layer and an inland push of easterly flow around 900 hPa, potentially associated with a mesoscale low.

REFERENCES

Collis, S., A. Protat, P. May, and C. Williams 2013: Statistics of storm updraft velocities from TWP-ICE including verification with profiling measurements. *J. Appl. Meteor. Climatol.,* **52,** 1909-1922.

Davies-Jones, R. , 1984: Streamwise vorticity: The origin of updraft rotation in supercell storms. *J. Atmos. Sci.,* **41,** 2991–3006.

Markowski, P. M., 2002: Hook echoes and rear-flank downdrafts: A review. *Mon. Wea. Rev.,* **130,** 852–876.

Markowski, P. M., J. M. Straka, E. N. Rasmussen, R. P. Davies-Jones, Y. Richardson, and J. Trapp, 2008: Vortex lines within low-level mesocyclones obtained from pseudo-dual-Doppler radar observations. *Mon. Wea. Rev.,* **136,** 3513–3535.

Markowski, P. M., and Y. P. Richardson, 2014: The influence of environmental low-level shear and cold pools on tornadogenesis: Insights from idealized simulations. *J. Atmos. Sci,* **71,** 243-275.

Moller, A. R., C. A. Doswell III, and R. Przybylinski, 1990: High precipitation supercells: A conceptual model and documentation. Preprints, *16th Conf. on Severe Local Storms,* Kananaskis Park, Alberta, Canada, Amer. Meteor. Soc., 52–57.

Protat, A., and I. Zawadzki, 1999: A variational method for real-time retrieval of three-dimensional wind field from multiple-Doppler bistatic radar network data. *J. Atmos. Oceanic Technol.,* **16,** 432–449.